Inst. Phys. Conf. Ser. No 148
Paper presented at Applied Superconductivity, Edinburgh, 3–6 July 1995

DC SQUIDS based on YBaCuO nanobridges

M.V. Pedyash, D.H.A. Blank and H. Rogalla

Low Temperature Division, Department of Applied Physics, University of Twente, P.O.Box 217, 7500 AE Enschede, The Netherlands.

Abstract. DC SQUIDs based on YBaCuO thin film nanobridges have been investigated. Critical current densities J_c are up to $3\cdot10^6$ A/cm^2 at T=77 K and follow $J_c \propto (1-T/T_c)^{1.6\pm0.1}$. High values of the voltage-flux modulation are observed (8 μV peak to peak at 77 K). A temperature dependence of the SQUID modulation found to be essentially different from the one of the conventional weak link SQUID. We discuss our devices by considering degradation of the nanobridge area during structuring, which leads to a transition from SNS to SS'S type junction with decreasing temperature.

1. Introduction

Most high-T_c SQUIDs are based on grain boundary weak links or ramp type junctions. The techniques to prepare such structures have been developed extensively and often face technological problems caused by an extremely short coherence length ξ. Recent results show that nanobridges, although having dimensions significantly exceeding ξ, manifest a true Josephson behaviour and are suitable for SQUID fabrication [1-3]. The concept of the coherent motion of flux quanta has become a standard for nanobridges description, and explains a wide variety of effects [4]. However, the periodic supercurrent-phase relation, which lays in the SQUID operation principle, does not follow from this model.

We investigated SQUIDs based on high-T_c thin film nanobridges systematically. We explain the Josephson nature of these devices by considering degradation of the bridge area during structuring, which leads to a transition from SNS to SS'S type junction with decreasing temperature.

2. Experimental

SQUIDs were structured in 50 nm thick $YBa_2Cu_3O_{7-\delta}$ films by, both, electron beam lithography (EBL) and direct focused ion beam milling (FIB). An inductively shunted dc SQUID geometry was chosen. A patterning procedure and SQUID geometry are discussed elsewhere [3]. T_c of unstructured films is (90±1) K. The superconducting transition curves R(T) of the investigated devices show the presence of a "foot" that grows rapidly with the decrease of the bridge width w, starting from w≈250 nm (inset in fig. 1). For wider bridges no degradation of T_c has been observed. The current voltage characteristics (I-V) of SQUIDs at zero external magnetic field (fig. 1) are similar to those of single nanobridges discussed elsewhere [5]. On the same substrate the critical current I_c is a linear function of the nanobridge width w for 50 nm < w < 350 nm. The critical current density J_c is up to $3 \cdot 10^6$ A/cm^2 at 77 K and follows $J_c \propto (1-T/T_c)^{1.6\pm0.1}$ in a wide range of temperatures from T_c down to at least $T_c/2$.

For w< 300 nm voltage-flux modulation was observed in our SQUIDs. The maximum detected peak to peak voltage modulation U_{mod} is 8 μV at 77K for the device based on 250 nm bridges (fig. 2) and 45 μV at 4.2 K (100 nm bridges). From the period of the voltage-flux modulation B_0 the SQUID effective sensing area $A_{eff}=\Phi_0/B_0$ is calculated. A_{eff} is 0.07 mm^2 at 4.2 K and grows at higher temperatures (fig. 3). For the inductively shunted SQUID with the pick-up loop much larger than the SQUID loop, flux in the SQUID can be written: $\Phi=B \cdot A_p L_{sq}/L_p$, where A_p is the pick-up loop area, L_p is the pick-up loop inductance and L_{sq} is the inductance of the SQUID loop. L_{sq} estimated to be 20 pH at T=4.2 K. We assume that A_p and L_p depend on geometry of the device but not on temperature. Both, kinetic and geometrical terms of the SQUID inductance are functions of the magnetic field penetration depth λ(T) [6]. Assuming $\lambda(T)=\lambda_0/(1-(T/T_c)^2)^{1/2}$, where λ_0 is the penetration depth at zero temperature, the experimental data can be fitted with λ_0=180 nm (the drawn line in fig. 3).

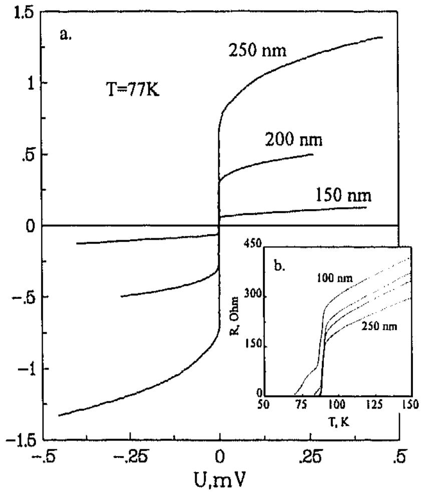

Fig. 1. The I(V) (a) and R(T) (b) characteristics of SQUIDs with nanobridges of different width.

The temperature dependence of the voltage modulation $U_{mod}(T)$ is essentially different from the one of conventional weak link SQUIDs described by the RSJ model. For wider bridges, with decreasing temperature starting from T_c of bulk, the amplitude of the modulation increases rapidly, and reaches quite a narrow maximum at $T \approx 0.9T_c$. With further decrease of temperature the amplitude of modulation drops and vanishes. Narrow bridges, where T_c is suppressed significantly, show decrease of the voltage modulation at intermediate temperatures and fast increase at temperatures around 4.2 K (fig. 5, 6a). This behaviour can not be explained by increase of the SQUID screening parameter $\beta_L=2I_cL_{sq}/\Phi_0$

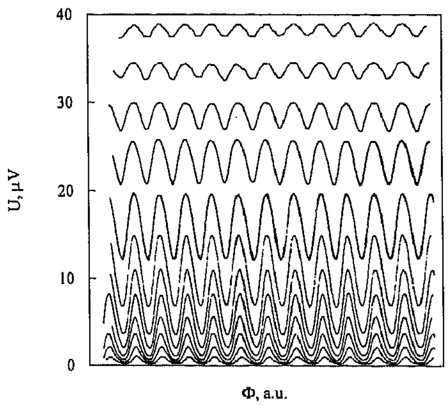

Fig. 2. The voltage-flux modulation of the SQUID based on 250 nm wide bridges at different bias voltages (T=77.4K).

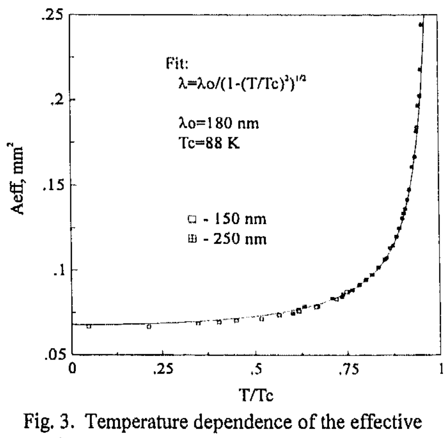

Fig. 3. Temperature dependence of the effective sensing area A_{eff} of two different SQUIDs. The solid line is the model fit (see text).

with decreasing temperature. The increase of β_L leads to a saturation of the modulation amplitude and not to a suppression.

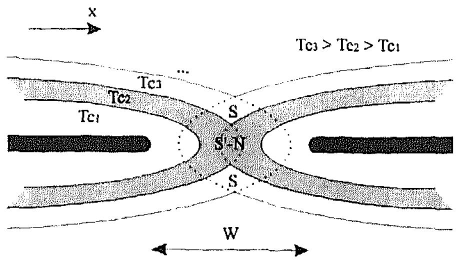

Fig. 4. *Schematic critical temperature distribution* inside the nanobridge area.

3. Discussion

It is natural to assume that superconducting properties of YBaCuO change in the vicinity of a trench patterned by either FIB or EBL. Earlier experiments demonstrated that a superconductor shows degradation of T_c after irradiation by high energy ions [7]. We assume the spatial distribution of T_c in a region close to the trench follows the empirical formula:

$$T_c(x)=T_{cb}(1-e^{X/X_0}), \qquad (1)$$

where T_{cb} is the critical temperature of bulk, x is the distance from the trench and x_0 is the characteristic length of T_c variation. Applying this formula to our nanobridge, we expect an evolution of R(T) if the width w goes to $2x_0$. This is confirmed by our experimental results, if take x_0 in the order of 50 nm.

A nanobridge can be considered as an SNS type junction in the temperature range $T_{c2} < T < T_{c3}$, and as an all-superconductor below T_{c2}, where T_{c2} is the critical temperature of the central region of the bridge, and T_{c3} is T_c of the layer next to it (fig. 4). Both, T_{c2} and T_{c3} are functions of the bridge width w. Such system can be described by the "two fluid" model, where the Josephson component of the supercurrent I_{jos} is gradually substituted by a "strong" (i.e. non-periodic with the phase difference $\Delta\varphi$) term with decreasing temperature. We calculated the temperature dependence I_{jos} according to Likharev and Kupriyanov [8, 9], assuming T_c of the bridge is given by (1), see figure 6c. The SQUID voltage modulation is proportional to the critical current I_c (assumed to be the Josephson current) and can be written as [10]:

$$U_{mod}=\frac{7}{\pi^2}\cdot\frac{I_c R_n}{1+\beta_L}\left(1-3.57\frac{\sqrt{k_b T\cdot L_{sq}}}{\Phi_0}\right). \qquad (2)$$

This expression explains the vanishing of the nanobridge SQUID modulation at lower temperatures due to the Josephson term of the supercurrent declination. By assuming a T_c distribution along the bridge according to (1), the temperature range where the modulation is observed, can be calculated and agrees with the experiment for the bridges of all widths.

The difference between our SQUID and the conventional Josephson weak link device described by the RSJ model is that the nanobridge SQUID is the typical "flux-flow" device with the corresponding I-V characteristics (fig. 1). Instead of single and well defined RSJ like resistance parameter R_n, the nanobridge SQUID is characterised by the dynamic resistance R_{dyn}, which is determined by effects of vortex flow in the bridge and can depend on temperature in a rather sophisticated way. R_{dyn}, defined as the resistance of the SQUID at voltage bias where the SQUID modulation was recorded, was measured experimentally and raises strongly in, both, low and high temperature regions (fig. 5). By putting the approximation of the experimental values of R_{dyn} and the calculated $I_{jos}(T)$ into (2) the SQUID voltage modulation U_{calc} was calculated as a function of temperature for the bridges of different width (fig. 6b). A qualitative agreement between the experimental data and the calculated U_{calc} have been obtained for all temperatures and bridge widths (fig. 6).

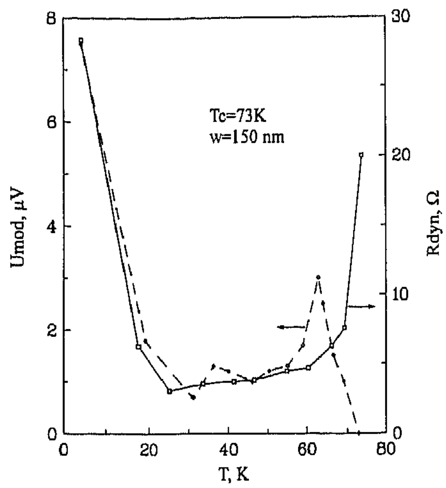

Fig. 5 The amplitude of SQUID voltage-flux modulation U_{mod} and the dynamic resistance R_{dyn} of SQUID (U_{bias}=10μV) as a function of temperature.

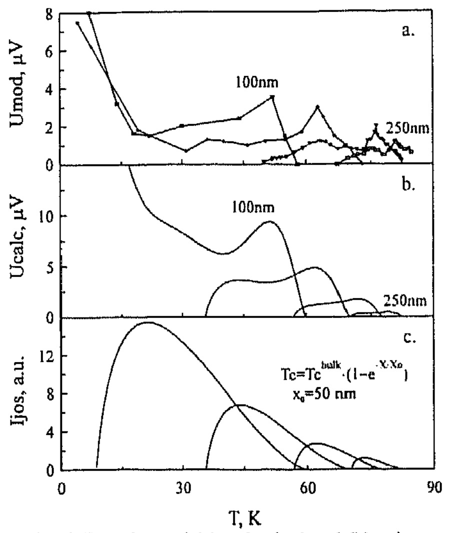

Fig. 6 Experimental (a) and calculated (b) values of U_{mod}(T) and calculated Josephson component of current (c) for SQUIDs with bridges of different w.

4. Concluding remarks

A more realistic assumption would be that even at high temperatures only a small fraction of total supercurrent in the bridge is of Josephson origin. This coincides with the high observed values of J_c at 77 K and explains why we did not see any significant suppression of I_c by a weak magnetic field.

The above discussion brings us to the idea that vortices in the nanobridge are not always of the pure Abrikosov type, but can gain properties of Josephson fluxons, like increasing of the vortex size and gradual disappearance of the normal vortex core with decreasing of w. This can explain the low value of the viscous drag coefficient η of vortex motion in a nanobridge [5]. The proposed $T_c(x)$ distribution near the bridge edge leads to a more complicated shape of the edge barrier for a vortex than assumed usually [4].

As has been mentioned, the effects of vortex flow in the bridge strongly determine the behaviour of the SQUID. Possibly, sharp maximum in U_{mod}(T) curve can be explained by the 3D to 2D vortex crossover in YBaCuO, or by freezing the vortex flow state into the glass state [11].

References

[1] S.E. Romaine et al., Appl. Phys. Lett., **59** (20), 2603 (1991)

[2] J. Schneider et al., Appl. Phys. Lett., **65** (19), 2475 (1994).

[3] D.H.A. Blank et al., to be published in IEEE Trans. on Appl. Sc., **5** No 2 or No 3 (1995)

[4] H. Rogalla, Habilitation thesis, University of Giessen, Germany (1986).

[5] M.V. Pedyash et al., to be published in IEEE Trans. on Appl. Sc., **5** No 2 or No 3 (1995)

[6] H. Hilgenkamp, Ph.D. thesis, University of Twente, the Netherlands, 1995.

[7] S.S. Tinchev, IEEE Trans. on Appl. Sc., vol. 3, No 1, 28 (1993).

[8] K.K. Likharev, Rev. of Mod. Phys., vol. 51, No 1, 109-115 (1979).

[9] M.Yu. Kupriyanov et al., Sov. Phys. JETP **56** (1), 235 (1982).

[10] K. Enpuku et al., J. Appl. Phys., **73**, 7929 (1993).

[11] P. Berghuis and P. Kes, Phys. Rev. B, **47**, 262 (1993).